



Room-temperature and solution-processed vanadium oxide buffer layer for efficient charge injection in bottom-contact organic field-effect transistors



Seokgeun Jin ^a, Byung Jun Jung ^b, Chung Kun Song ^a, Jeonghun Kwak ^{a,*}

^a Department of Electronic Engineering, Dong-A University, Busan 604-714, Republic of Korea

^b Department of Materials Science and Engineering, The University of Seoul, Seoul 130-743, Republic of Korea

ARTICLE INFO

Article history:

Received 30 June 2014

Received in revised form

19 September 2014

Accepted 18 October 2014

Available online 29 October 2014

Keywords:

Organic field-effect transistor

Contact resistance

Vanadium oxide

Buffer layer

ABSTRACT

We introduce a room temperature and solution-processible vanadium oxide (VO_x) buffer layer beneath Au source/drain electrodes for bottom-contact (BC) organic field-effect transistors (OFETs). The OFETs with the VO_x buffer layer exhibited higher mobility and lower threshold voltages than the devices without a buffer layer. The hole mobility with VO_x was over $0.11 \text{ cm}^2/\text{V}$ with the BC geometry with a short channel length ($10 \mu\text{m}$), even without a surface treatment on SiO_2 . The channel width normalized contact resistance was decreased from $98 \text{ k}\Omega \text{ cm}$ to $23 \text{ k}\Omega \text{ cm}$ with VO_x . The improved mobility and the reduced contact resistance were attributed to the enhanced continuity of pentacene grains, and the increased work function and adhesion of the Au electrodes using the VO_x buffer layer.

© 2014 Elsevier B.V. All rights reserved.

1. Introduction

Organic field-effect transistors (OFETs) have attracted considerable attention for decades owing to their potential application to low cost, transparent and flexible electronic devices [1–3]. Various electronic devices based on OFETs, such as radio frequency identification (RFID) tags, display backplanes, sensors, and integrated circuits (ICs) have been reported [2,3], but there is plenty of room for improvement in their performance toward practical applications. For the integration of these logic devices (e.g., inverters) as well as OFETs, it is advantageous to use the bottom-contact (BC) structure, in which the source (S)/drain (D) electrodes and insulator layer are aligned on the same plane with the induced channel. In addition, the small-scale S/D electrodes and wiring can be formed in BC devices by photolithography, whereas there is a limit to scaling down the channel length with a top-contact (TC) structure using fine metal shadow masks. Despite these merits, compared to TC OFETs, BC OFETs suffer from higher contact resistance (R_C) between the organic semiconductors and S/D electrodes [4–6]. In general, R_C originates not only from the energy barrier at the organic semiconductor/electrode interfaces, but also from the discontinuity in the grain growth of the organic semiconductor

between the channel region and electrodes [5,7]. Because S/D electrodes in BC OFETs are contiguous to the active channel region, the performance is strongly affected by R_C . To enhance the performance of the BC OFETs, it is essential to reduce the contact resistance by lowering the energy barrier. For this purpose, several methods for treating S/D electrodes have been reported, such as O_2 plasma [8], self-assembled monolayers (SAMs) with a dipole moment [9–11], and a few nanometer thick buffer layer with a transition metal oxide (TMO) [12–14], which can adjust the work function of S/D electrodes. In particular, the use of solution-processible TMOs is a favourable method because (i) they can be applied easily to all kinds of metals, (ii) their low process temperature is suitable for flexible or stretchable device fabrication, and (iii) they have deep highest-occupied-molecular-orbital (HOMO) and lowest-unoccupied-molecular-orbital (LUMO) energy levels that are sufficient to facilitate carrier injection into organic semiconductors [15–17].

In the present study, solution-processed VO_x was incorporated as a buffer layer in Au S/D electrodes for efficient charge injection in pentacene-based BC OFETs. The devices with the VO_x buffer layer showed higher hole mobility (μ) and lower threshold voltages (V_{th}) compared to the device without a VO_x buffer layer. The contact resistance was reduced significantly when the VO_x buffer layer was used. Furthermore, because the VO_x layer was formed at room temperature using a solution process, it is much easier to fabricate

* Corresponding author.

E-mail address: jkwak@dau.ac.kr (J. Kwak).

BC OFETs and improve their performances compared to other methods, such as a SAM treatment.

2. Experimental details

Vanadium(V)oxytriisopropoxide (Sigma Aldrich) was diluted in deionized water with volume ratios of 1:150, 1:200, and 1:250. To form the VO_x thin-films, the prepared solutions were spin-coated on the substrates at 2000 rpm, followed by a hydrolysis process in an ambient atmosphere for 30 min. The thickness of the VO_x films with 1:150, 1:200, and 1:250 volume ratios were 10, 7, and 5 nm, respectively. The optical, electrical, and morphological properties of the films were characterized by UV–Vis spectroscopy (Agilent Cary 50), photoelectron spectroscopy (Riken Keiki AC-2), and atomic force microscopy (AFM, TopoMetrix Explorer). The thickness was measured with a non-contact 3D surface profiler (Nanosystem NV-E1000).

Bottom-contact pentacene OFETs were fabricated on a 100 nm-thick SiO_2 dielectric layer that had been grown thermally on heavily-doped Si wafers. The measured capacitance (C_i) of SiO_2 was 33.3 nF/cm^2 . The wafers were cleaned using a conventional method prior to use. For the patterning of source–drain electrodes, we spin-coated a commercial photoresist (DTFR-525, Dongjin Semichem) at 1000 rpm for 40 s, followed by baking at 100°C for 2 min. After exposing the substrates to UV (365 nm , 10.6 mW/cm^2) through a patterned chrome mask, they were immersed in a diluted positive developer (DPD-200, Dongjin Semichem) for 30 s. Then, a 50-nm-

thick Au layer was evaporated thermally on the patterned substrates with or without a VO_x buffer layer. Finally, patterned source and drain electrodes were obtained by removing the residual photoresist layer (lift-off) using acetone. The OFETs consisted of various channel lengths (L) of 10, 20, 40 and $80 \mu\text{m}$ with a channel width (W) of $800 \mu\text{m}$. On the top of that, a 50 nm pentacene layer was deposited at a rate of 0.03 nm/s with a substrate temperature of 80°C . The transfer and output characteristics of the OFETs were measured in air using a semiconductor parameter analyzer (Keithley 4200).

3. Results and discussion

Fig. 1(a) shows the device structure of the BC OFETs with a 0–10 nm VO_x buffer layer. A VO_x layer was formed below the Au S/D electrodes because the field-induced current in OFETs mainly flows within a few monolayers of the pentacene molecules. X-ray photoelectron spectroscopy (XPS) data from previous reports [15,16] showed that both thermal evaporation of vanadium oxide and the hydrolysis of vanadium precursor are likely to form vanadium sub-oxide (VO_x) instead of vanadium pentoxide (V_2O_5) due to oxygen vacancies. The formation of VO_x with solution-process was verified by comparing the UV–Vis absorption spectrum with that of the thermally evaporated VO_x film, as shown in Fig. 1(b). They revealed similar spectra with a peak at 400 nm and an absorption edge at approximately 500 nm , showing that VO_x had been produced successfully via hydrolysis. The AFM image of solution-processed 10-nm-thick VO_x layer in Fig. 1(b) inset showed that VO_x grains had formed homogeneously with a good surface morphology (the root-mean-square roughness of 1.6 nm). The work function of VO_x was 5.2 eV which was 0.3 eV higher than that of pristine Au. Enhanced charge injection is expected with the VO_x buffer layer because the HOMO energy level of pentacene is approximately -5 eV .

Fig. 2(a) shows the transfer characteristics of OFETs ($L = 10 \mu\text{m}$) as a function of the thickness of the VO_x layer. All the devices with a VO_x layer exhibited an approximately one order of magnitude higher drain–source current (I_{DS}) than the device without the buffer layer. In particular, the device using 10 nm of VO_x showed the highest performance of all devices possessing different channel lengths. The OFETs with a thinner buffer layer showed similar but slightly lower performance to the best device. The hole mobility of the devices using the buffer layer ranged from 0.10 to $0.11 \text{ cm}^2/\text{V}$, whereas that of the control device was $0.02 \text{ cm}^2/\text{V}$. The OFETs with $L = 80 \mu\text{m}$ also exhibited improved mobility with the VO_x buffer layer ($\mu = 0.13 \text{ cm}^2/\text{V}$) compared to the control device ($\mu = 0.07 \text{ cm}^2/\text{V}$). Fig. 2(b) shows the output curves measured at the gate–source voltage (V_{GS}) of -30 V as a function of the VO_x thickness. When the buffer layer was used, all devices showed good output characteristics with high I_{DS} . On the other hand, low I_{DS} and S-shaped curves at the low drain–source voltage (V_{DS}) region were observed in the device without a buffer layer, meaning that the R_{C} was high in this device. The channel width normalized contact resistance ($R_{\text{C}}W$) was extracted using gated-transmission line method (TLM) [18]. For this, OFETs with various L values of 10, 20, 40 and $80 \mu\text{m}$ were fabricated and characterized. The total resistance normalized by the channel width ($R_{\text{total}}W$) at the linear regime ($V_{\text{DS}} = -5 \text{ V}$) was then calculated using the following equation:

$$R_{\text{total}}W = R_{\text{ch}}W + R_{\text{C}}W = \frac{L}{\mu C_i (V_{\text{GS}} - V_{\text{th}})} + R_{\text{C}}W \quad (1)$$

where R_{ch} is the channel resistance. The $R_{\text{C}}W$ values of the OFETs depending on the VO_x thickness were extracted from the $R_{\text{total}}W$ values of the devices at $V_{\text{GS}} = -30 \text{ V}$ as a function of L and their

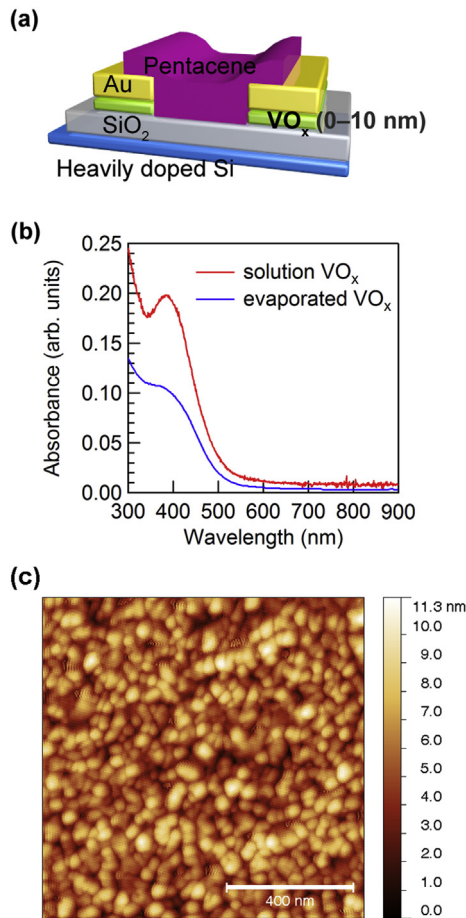


Fig. 1. (a) Device structure of the pentacene-based BC OFETs with 0–10 nm of VO_x buffer layer. (b) UV–Vis absorption spectra of solution-processed VO_x and thermal evaporated VO_x thin-films. (c) Surface morphology of the solution-processed VO_x layer (10 nm) measured by the AFM.

Download English Version:

<https://daneshyari.com/en/article/1785928>

Download Persian Version:

<https://daneshyari.com/article/1785928>

[Daneshyari.com](https://daneshyari.com)